Chemistry—A European Journal

Supporting Information

Selective One-Pot Syntheses of Mixed Silicon-Germanium Heteroadamantane Clusters

Benedikt Köstler, Michael Bolte, Hans-Wolfram Lerner, and Matthias Wagner*

1. Experimental Details and Characterization Data

1.1 General Considerations. All reactions were carried out under an inert-gas atmosphere (dry argon or nitrogen) using standard Schlenk or glove-box techniques. Commercially available starting materials were used as received. CH_2Cl_2 was dried over CaH_2 and freshly distilled prior to use; CD_2Cl_2 was stored over molecular sieve (3 Å). NMR spectra were recorded on a Bruker Avance III HD 500 spectrometer equipped with a Prodigy BBO 500 S1 probe. $^{1}H/^{13}C\{^{1}H\}$ NMR spectra were referenced against (residual) solvent signals (CD_2Cl_2: 5.32 ppm/53.84 ppm;[1] s = singlet). $^{29}Si\{^{1}H\}$ NMR spectra were calibrated against external $Si(CH_3)_4$ ($\delta(^{29}Si) = 0$); whenever present, $SiCl_4$ ($\delta(^{29}Si) = -18.9$ ppm) was used as internal standard. Elemental analyses were performed at the microanalytical laboratory Pascher, Remagen, Germany. UV/Vis absorption spectra were recorded at room temperature using a *Varian* Cary 60 Scan UV/Vis spectrophotometer.

1.2 Formal considerations regarding the formation of heteroadamantanes [0], [1], and [2] from Me_2GeCl_2, Si_2Cl_6, and [*n*Bu_4N]Cl

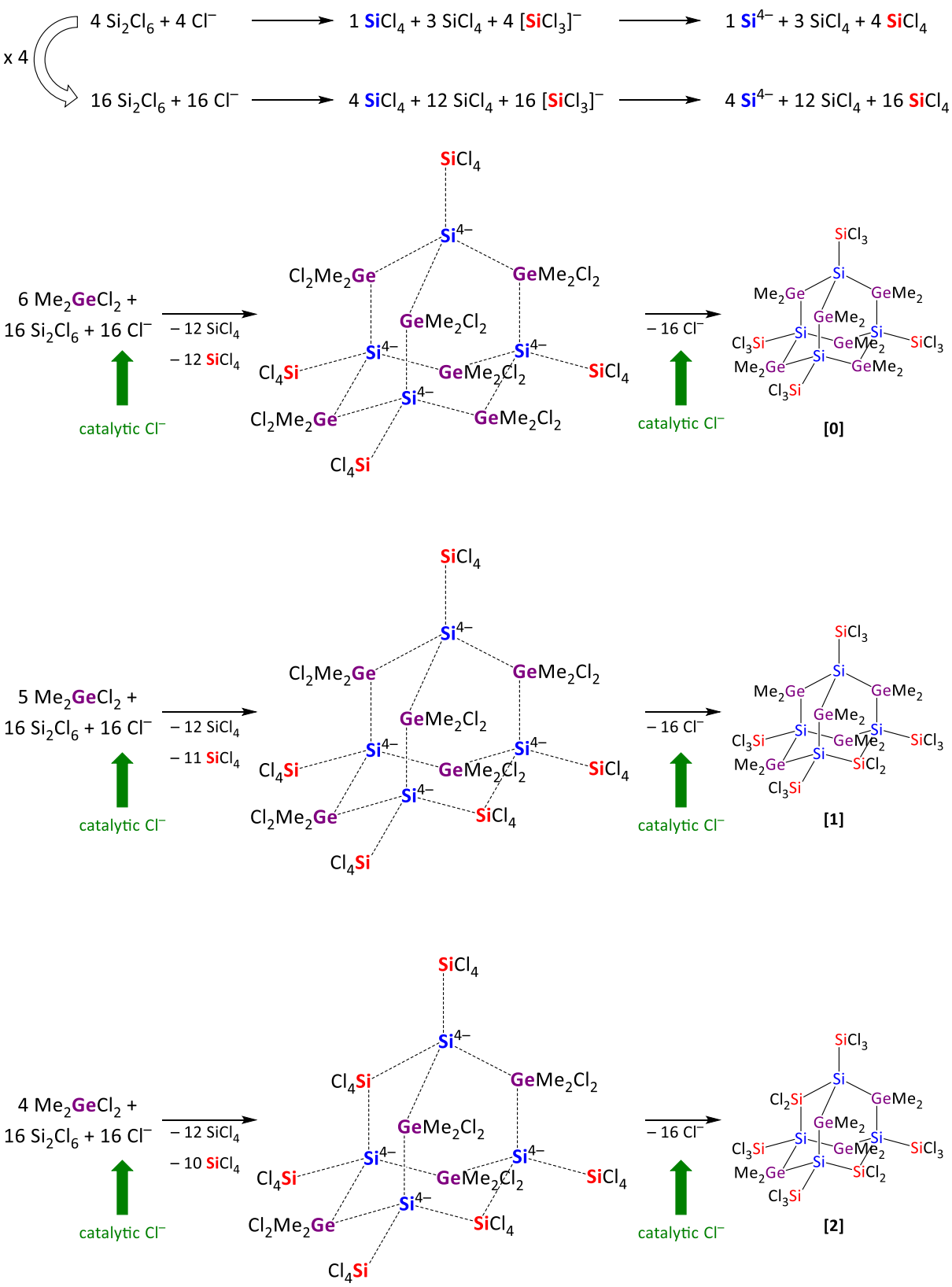

Figure S1. Balanced reaction equations and formal atom and electron count for the formation of heteroadamantanes **[0]**, **[1]**, and **[2]** from Me_2GeCl_2, Si_2Cl_6, and Cl^-.

For a better understanding of the formation of the heteroadamantanes **[0]**, **[1]**, and **[2]**, the following considerations regarding the atom and electron balance are helpful, but are explicitly **not** meant to be a mechanistic proposal: The Cl^{-}-induced disproportionation of Si_2Cl_6 releases the transient silanide $[SiCl_3]^{-}$ together with the byproduct $SiCl_4$. 4 $[SiCl_3]^{-}$ anions can formally abstract 4 Cl^{+} cations from 1 $SiCl_4$ molecule, generating 1 $[Si]^{4-}$ tetraanion and 4 $SiCl_4$ molecules. Accordingly, 16 Si_2Cl_6 and 16 Cl^{-} ions are required to generate 4 $[Si]^{4-}$ anions (and 28 $SiCl_4$ as byproducts).

In the case of **[0]**, each of these 4 $[Si]^{4-}$ anions is formally incorporated in the heteroadamantane core *via* 3 nucleophilic substitution reactions on Me_2GeCl_2 and 1 nucleophilic substitution reaction on $SiCl_4$, which is present in large supply. In summary, 6 Me_2GeCl_2, 4 $SiCl_4$, and 4 $[Si]^{4-}$ anions are consumed in the formation of 1 molecule of **[0]**; the total number of 16 Cl^{-} ions released renders the overall reaction catalytic in Cl^{-}.

In the cases of **[1]** or **[2]**, the formal processes remain the same, apart from the fact that 1 or 2 $SiCl_4$ molecule(s) are incorporated instead of 1 or 2 Me_2GeCl_2 molecule(s).

N*ote:* The compound numbers **[X]** refer to the number X of $SiCl_2$ vertices that are incorporated instead of $GeMe_2$ vertices (ideal number of the latter: 6 in **[0]**).

1.3 Synthesis of [0]

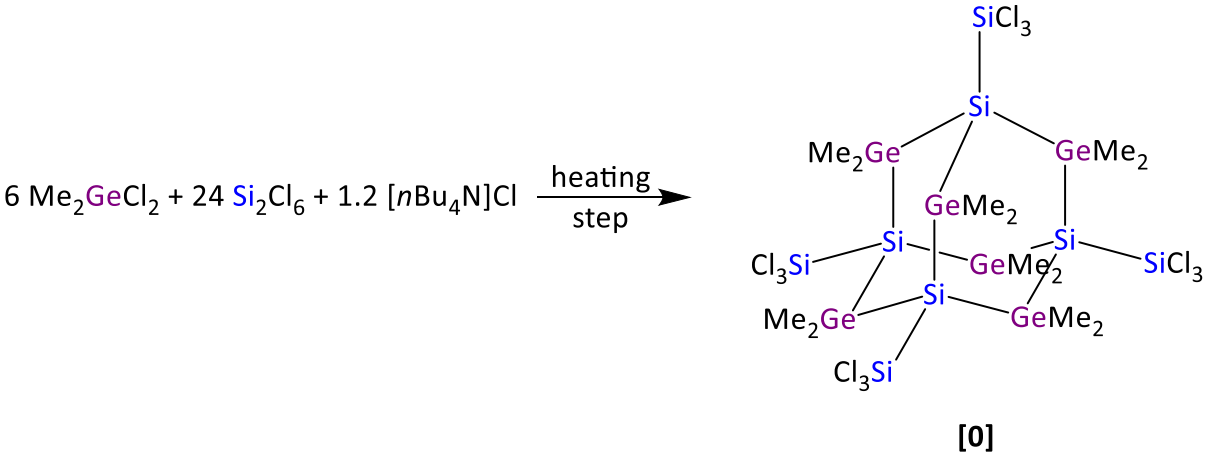

[0]

A solution of [*n*Bu$_4$N]Cl (0.320 g, 1.15 mmol) and Me_2GeCl_2 (1.000 g, 5.76 mmol) in CH_2Cl_2 (20 mL) was prepared in an 100 mL Schott glass bottle in the glove box. Neat Si_2Cl_6 (6.200 g, 23.05 mmol) was added at room temperature. The bottle was closed and stored in the glove box for 4 h. The screw cap was removed and all volatiles were slowly evaporated overnight to obtain a colorless, solid residue.*) An ampoule was charged with this solid and CH_2Cl_2 (10 mL). The ampoule was flame-sealed under reduced pressure and heated to 60 °C for 6 d to guarantee complete conversion. During this time, colorless, needle-shaped crystals of **[0]** grew from the reaction solution. The ampoule was opened in the glove box, the crystals were isolated by filtration, and washed with CH_2Cl_2 (3 × 0.5 mL). Yield of single-crystalline **[0]**: 300 mg (0.24 mmol, 25%). All volatiles were removed from the combined filtrates under reduced pressure, and the colorless, sticky residue was washed with CH_2Cl_2 (4 × 0.5 mL) to obtain a microcrystalline second fraction of **[0]** (232 mg, 0.18 mmol, 19%) that was of comparable purity to the first crop (NMR spectroscopic control). Overall yield of **[0]**: 532 mg (0.42 mmol, 44%).

*) *Note:* At this stage, the formation of **[1]** and **[2]** (see below) was proven by NMR spectroscopy, whereas no **[0]** was detected.

Heteroadamantane **[0]** was characterized by single crystal X-ray diffraction (triclinic, *P*-1), NMR spectroscopy, elemental analysis, and UV/Vis spectroscopy.

^{1}H NMR (500.2 MHz, CD_2Cl_2, 298 K): δ = 0.91 ppm (s, 36 H; $GeMe_2$).

^{13}C{^{1}H} NMR (125.8 MHz, CD_2Cl_2, 298 K): δ = 2.6 ppm ($GeMe_2$).

^{29}Si{^{1}H} NMR (99.4 MHz, CD_2Cl_2, 298 K): δ = 16.2 ($SiCl_3$), –83.4 ppm (*Si*–$SiCl_3$).

Elemental analysis: Calculated for $C_{12}H_{36}Cl_{12}Ge_6Si_8$ (1266.28): C 11.38; H 2.87. Found: C 11.93; H 2.85.
UV/vis (cyclohexane): λ_{max} (ε) = 205 (1.0×10^5), 234 nm (1.3×10^5 $mol^{-1}dm^3cm^{-1}$); λ_{onset} = 285 nm; E_G^{opt} = 4.35 eV (see Table S2 and Figure S16).

The synthesis of **[0]** was also performed with the formally required ideal stoichiometry of 6 Me_2GeCl_2 : 16 Si_2Cl_6 : cat. [*n*Bu_4N]Cl (cf. Figure S1): Me_2GeCl_2 (0.500 g, 2.88 mmol), Si_2Cl_6 (2.090 g, 7.77 mmol), [*n*Bu_4N]Cl (0.216 g, 0.78 mmol), and CH_2Cl_2 (10 mL). We reproducibly obtained lower yields of only ≈ 20%.

Note: Evaporation of all volatiles prior to heating is a crucial step for the successful synthesis of **[0]**, as became obvious from the following test reaction: An NMR tube was charged with the optimal 6:24:1.2-mixture of Si_2Cl_6, Me_2GeCl_2, and [*n*Bu_4N]Cl in CD_2Cl_2 and flame-sealed under reduced pressure. After heating to 60 °C for 3.5 d, no heteroadamantane **[0]** was formed, as proven by NMR spectroscopy.

1.4 Synthesis of [2]

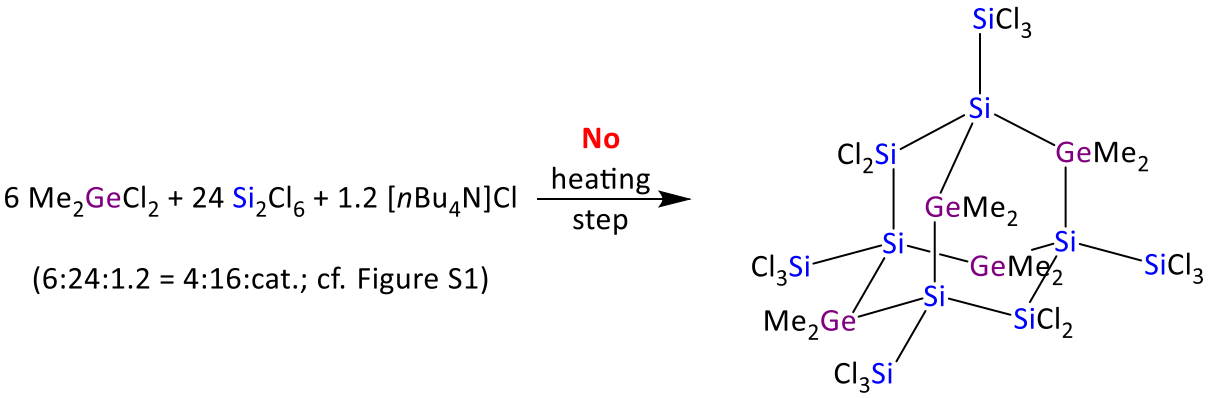

[2]

A solution of [*n*Bu$_4$N]Cl (0.160 g, 0.58 mmol) and Me$_2$GeCl$_2$ (0.500 g, 2.88 mmol) in CH$_2$Cl$_2$ (10 mL) was prepared in an 100 mL Schott glass bottle in the glove box. Neat Si$_2$Cl$_6$ (3.092 g, 11.50 mmol) was added at room temperature. The bottle was closed and stored in the glove box for 13 d to allow slow crystallization of **[2]**.*) The crystals were isolated by filtration and washed with CH$_2$Cl$_2$ (1 mL) to obtain **[2]** as colorless crystals. Yield: 254 mg (0.20 mmol, 28%).

*) *Note:* Already after about 3 d, crystals of **[2]** were visible in the reaction vessel. The crystallization time of 13 d is the empirically determined optimum in terms of the obtained yield of **[2]** *vs*. contamination with co-crystallized **[1]** (cf. synthesis of **[1]**, Method B). **[2]** crystallizes first as the solubilities of the heteroadamantanes in CH$_2$Cl$_2$ follow the qualitative trend **[2]** < **[1]** < **[0]**.

Heteroadamantane **[2]** was characterized by single crystal X-ray diffraction (trigonal, *R*-3:H), NMR spectroscopy, elemental analysis, and UV/Vis spectroscopy.

^{1}H NMR (500.2 MHz, CD$_2$Cl$_2$, 298 K): δ = 1.03 ppm (s, 24 H; GeMe$_2$).

^{13}C{^{1}H} NMR (125.8 MHz, CD$_2$Cl$_2$, 298 K): δ = 1.6 ppm (GeMe$_2$).

^{29}Si{^{1}H} NMR (99.4 MHz, CD$_2$Cl$_2$, 298 K): δ = 29.6 (SiCl$_2$), 11.9 (SiCl$_3$), –81.0 ppm (*Si*–SiCl$_3$).

Elemental analysis: Calculated for C$_8$H$_{24}$Cl$_{16}$Ge$_4$Si$_{10}$ (1258.85): C 7.63; H 1.92. Found: C 7.15; H 1.80.

UV/vis (cyclohexane): see Table S2 and Figure S18.

Variation of the stoichiometry: The highest yields of **[2]** were obtained with the theoretically required stoichiometry of 6:24:1.2 = 4:16:0.8 (Me_2GeCl_2 : Si_2Cl_6 : [nBu$_4$N]Cl; cf. Figure S1). When the reaction was performed according to the same protocol but with fewer equivalents of Si_2Cl_6/Cl^- (6:8:0.8 or 6:12:1.2), none of the three heteroadamantanes, **[2]**, **[1]**, or **[0]**, was formed (NMR spectroscopic control). More equivalents of Si_2Cl_6/Cl^- (6:48:2.4) resulted in a mixture of heteroadamantane **[2]** and **[1]** with a combined yield of only ≈ 10%.

1.5 Synthesis of [0] by skeletal rearrangement of [2]

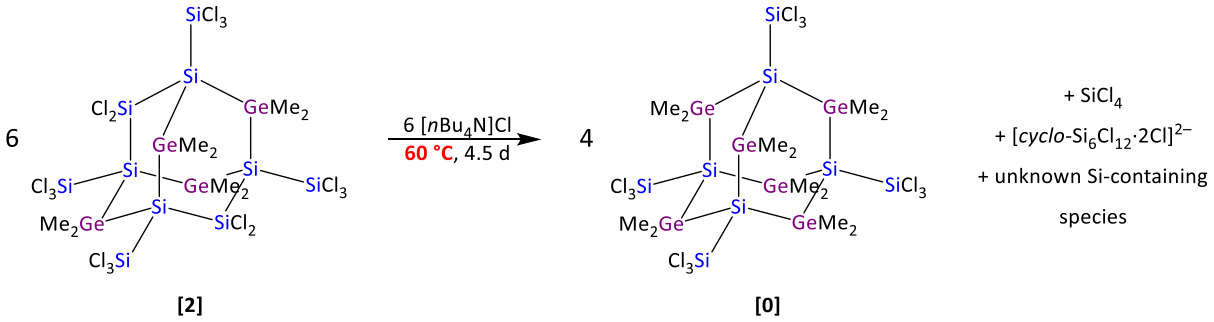

An ampoule was charged with **[2]** (0.350 g, 0.28 mmol), [*n*Bu$_4$N]Cl (0.080 g, 0.28 mmol), and CH_2Cl_2 (15 mL) and flame-sealed under reduced pressure. After heating to 60 °C for 4.5 d, the ampoule was opened, and all volatiles were removed under reduced pressure. The colorless, sticky residue was washed with CH_2Cl_2 (1.5 mL) to obtain **[0]** as a colorless solid. Yield: 118 mg (0.09 mmol, 50%).

Note: The reaction was also performed in a flame-sealed NMR tube (CD_2Cl_2) to identify the silicon-containing byproducts and to estimate the time required for the reaction on a preparative scale. According to ^{1}H and ^{13}C{^{1}H} NMR spectroscopy, **[0]** was the only methyl-containing product.

1.6 Synthesis of [1]

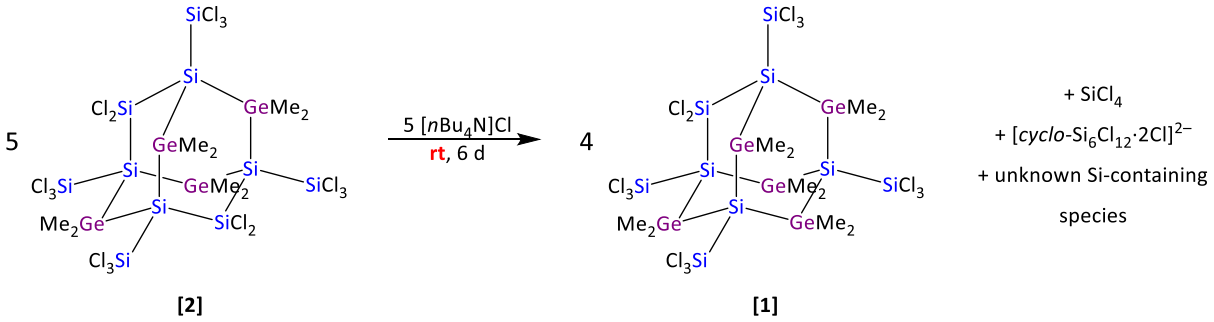

Method A: A solution of **[2]** (0.200 g, 0.16 mmol), [*n*Bu$_4$N]Cl (0.044 g, 0.16 mmol), and CH_2Cl_2 (10 mL) was prepared in a Schlenk flask and stirred at room temperature for 6 d. All volatiles were removed under reduced pressure and the colorless solid residue was washed with CH_2Cl_2 (4 mL) to obtain **[1]** as a colorless solid. Yield: 90 mg (0.07 mmol, 54%).

Note: The reaction was also performed in a flame-sealed NMR tube (CD_2Cl_2) to identify the silicon-containing byproducts and to estimate the time required for the reaction on a preparative scale. According to ^{1}H and ^{13}C{^{1}H} NMR spectroscopy, **[1]** was the only methyl-containing product.

Method B: A solution of [*n*Bu$_4$N]Cl (0.160 g, 0.58 mmol) and Me_2GeCl_2 (0.500 g, 2.88 mmol) in CH_2Cl_2 (10 mL) was prepared in a 100 mL Schott glass bottle in the glove box. Neat Si_2Cl_6 (3.092 g, 11.50 mmol) was added at room temperature. The bottle was closed and stored in the glove box for 20 d. During this time, colorless crystals grew from the reaction solution, which were isolated by filtration and washed with CH_2Cl_2 (5 mL). According to ^{1}H NMR spectroscopy, the crystals consisted of a mixture of **[1]** and **[2]** (ratio = 63:37). Yield: 285 mg (≈ 35% **[1]** + **[2]**).

Note: The **[1]**/**[2]** mixture obtained can subsequently be quantitatively converted to **[1]** by treatment with [*n*Bu$_4$N]Cl in CH_2Cl_2 (cf. Method A).

Heteroadamantane **[1]** was characterized by single crystal X-ray diffraction (orthorhombic, *Cmc*2_1), NMR spectroscopy, and UV/Vis spectroscopy. Pairs of corresponding ^{1}H and ^{13}C{^{1}H} NMR signals were identified by ^{13}C/^{1}H HSQC NMR spectroscopy and assigned the same color.

^{1}H NMR (500.2 MHz, CD_2Cl_2, 298 K): δ = 1.00 (s, 12 H; $GeMe_2$), 0.94 (s, 12 H; $GeMe_2$), 0.93 ppm (s, 6 H; $GeMe_2$).

^{13}C{^{1}H} NMR (125.8 MHz, CD_2Cl_2, 298 K): δ = 2.6 ($GeMe_2$), 2.2 ($GeMe_2$), 2.0 ppm ($GeMe_2$).

^{29}Si{^{1}H} NMR (99.4 MHz, CD_2Cl_2, 298 K): δ = 31.0 ($SiCl_2$), 16.2 ($SiCl_3$), 12.1 ($SiCl_3$), –80.7 (*Si*–$SiCl_3$), –83.3 ppm (*Si*–$SiCl_3$).

UV/vis (cyclohexane): see Table S2 and Figure S17.

1.7 Stepwise skeletal rearrangement of [2] *via* [1] to [0]

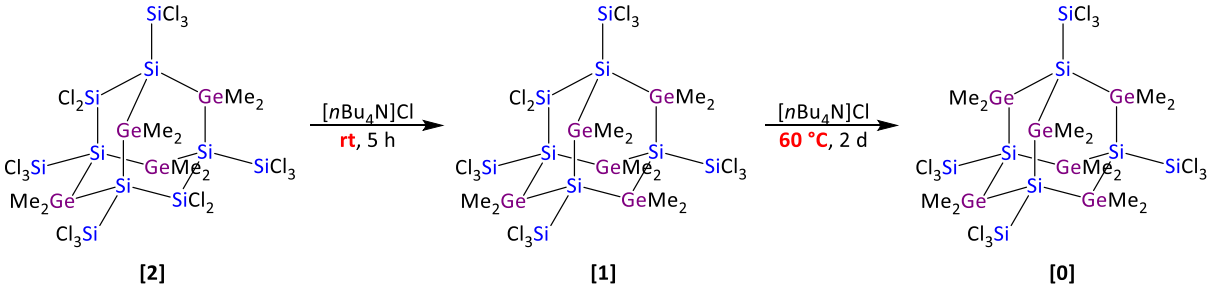

An NMR tube was charged with **[2]** (0.010 g, 0.008 mmol), [*n*Bu$_4$N]Cl (0.002 g, 0.008 mmol), and CD_2Cl_2 (0.5 mL) and flame-sealed under reduced pressure. Reaction progress was monitored by ^{1}H, $^{13}C\{^{1}H\}$, and $^{29}Si/^{1}H$ HMBC NMR spectroscopy. Spectra were recorded after 5 h, 3 d, and 6 d at room temperature and after subsequent heating to 60 °C for 2 d. The spectra revealed the stepwise rearrangement of **[2]** *via* **[1]** to **[0]** (cf. Figure S2): After 5 h, the NMR spectra showed **[1]** as the main product with small amounts of unconsumed **[2]** still present. After 3 d, the conversion to **[1]** was complete with no **[2]** or **[0]** present. After 6 d, small amounts of **[0]** had formed, but **[1]** still remained by far the main component. Complete conversion to **[0]** was achieved by heating the sample to 60 °C for 2 d (note that **[0]** was not converted further under these conditions).

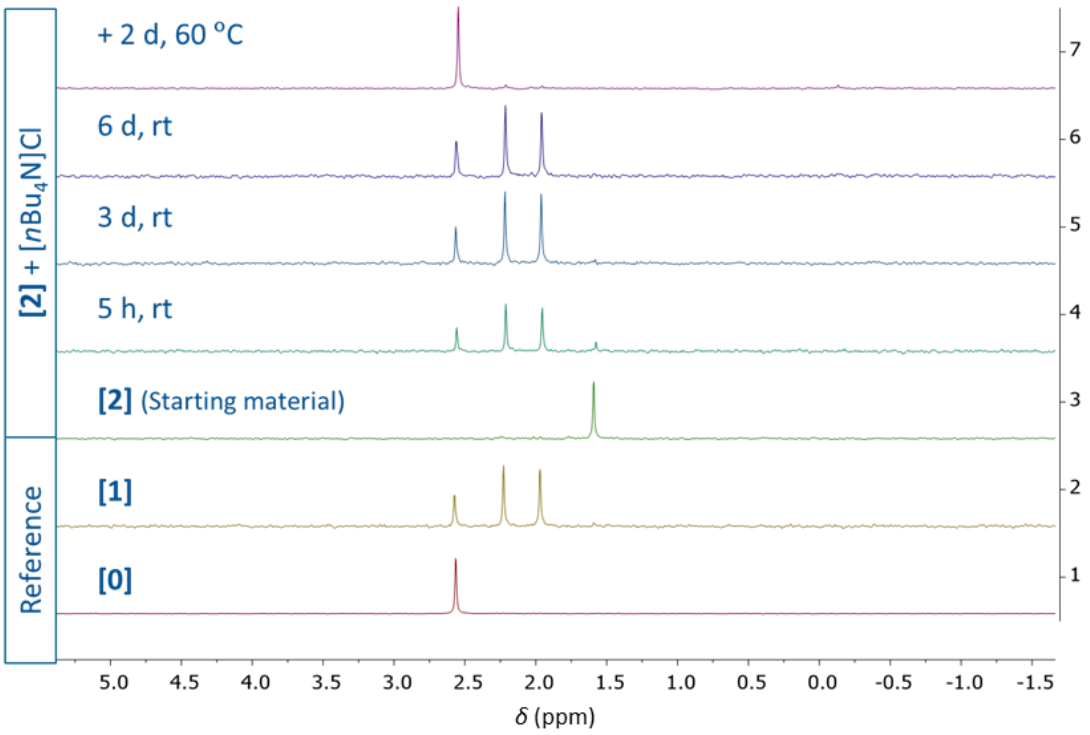

Figure S2. $^{13}C\{^{1}H\}$ NMR spectra recorded on the reaction mixture of **[2]** with 1 eq. of [*n*Bu$_4$N]Cl after 5 h, 3 d, and 6 d at room temperature and after subsequent heating of the sample to 60 °C for 2 d. Reference spectra of **[0]** and **[1]** are shown for comparison.

1.8 Attempts at the conversion of [0] to [1] by reaction of [0] with [*n*Bu$_4$N]Cl and either SiCl$_4$ or Si$_2$Cl$_6$

With the aim of investigating the reverse reaction from **[0]** to **[1]** (or **[2]**) through formal replacement of GeMe$_2$ by SiCl$_2$ vertices, four test experiments were performed (Table S1, entries a–d). In each case, we used 10 mg of heteroadamantane **[0]** in CD_2Cl_2 in a flame-sealed NMR tube. In none of these cases, a reaction occurred, neither at room temperature nor after heating to 60 °C. It is noteworthy in this context that we also found it impossible to introduce a third SiCl$_2$ vertex into **[2]** (and thereby generate a heteroadamantane "**[3]**") by treating **[2]** with a mixture of [*n*Bu$_4$N]Cl and Si$_2$Cl$_6$ in CD_2Cl_2 (Table S1, entry e).

Table S1. Treatment of **[0]** or **[2]** with [*n*Bu$_4$N]Cl and either SiCl$_4$ or Si$_2$Cl$_6$ leads to no reaction.

entry	hetero-adamantane	[*n*Bu$_4$N]Cl	SiCl$_4$	Si$_2$Cl$_6$	temperature	result
a	**[0]**	1 eq.	-	-	rt or 60 °C	no reaction
b	**[0]**	-	4 eq.	-	rt or 60 °C	no reaction
c	**[0]**	1 eq.	4 eq.	-	rt or 60 °C	no reaction
d	**[0]**	1 eq.	-	4 eq.	rt or 60 °C	no reaction
e	**[2]**	1 eq.	-	4 eq.	rt or 60 °C	no reaction

2. Plots of ^{1}H, $^{13}C\{^{1}H\}$, $^{29}Si\{^{1}H\}$, and $^{29}Si/^{1}H$ HMBC NMR spectra

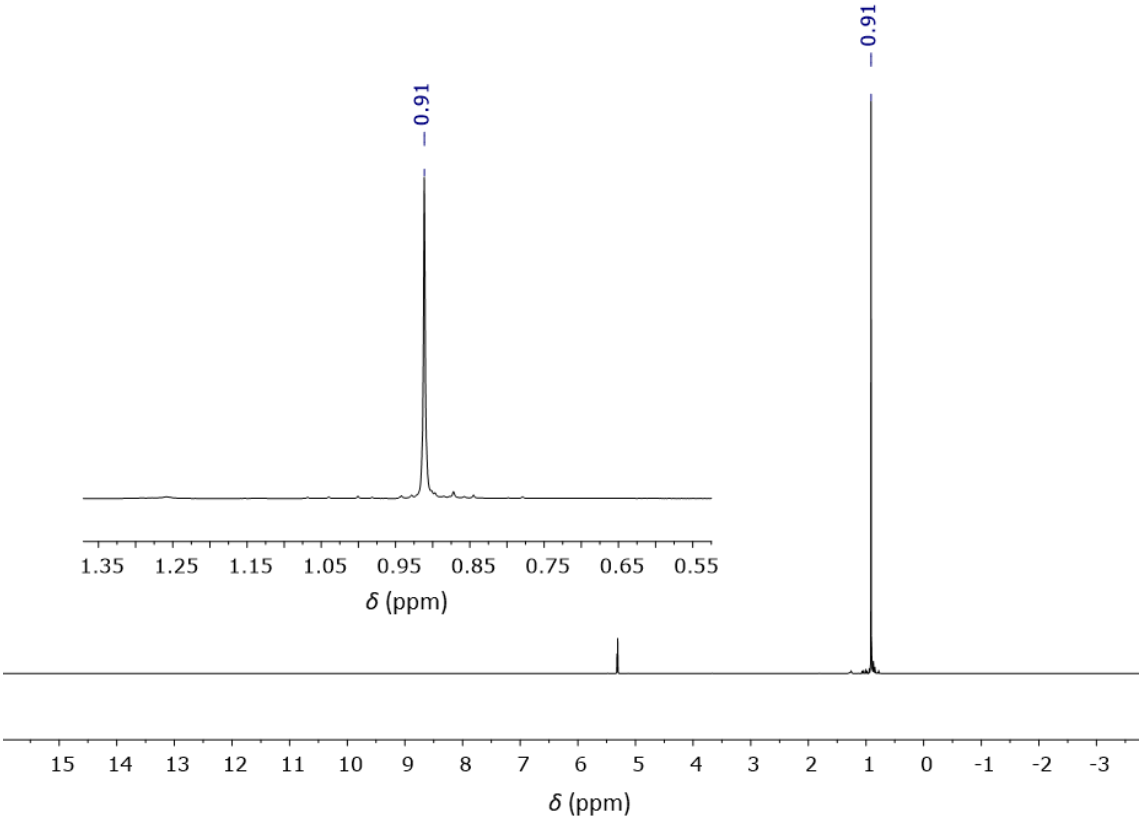

Figure S3. ^{1}H NMR spectrum of **[0]** (CD_2Cl_2, 500.2 MHz).

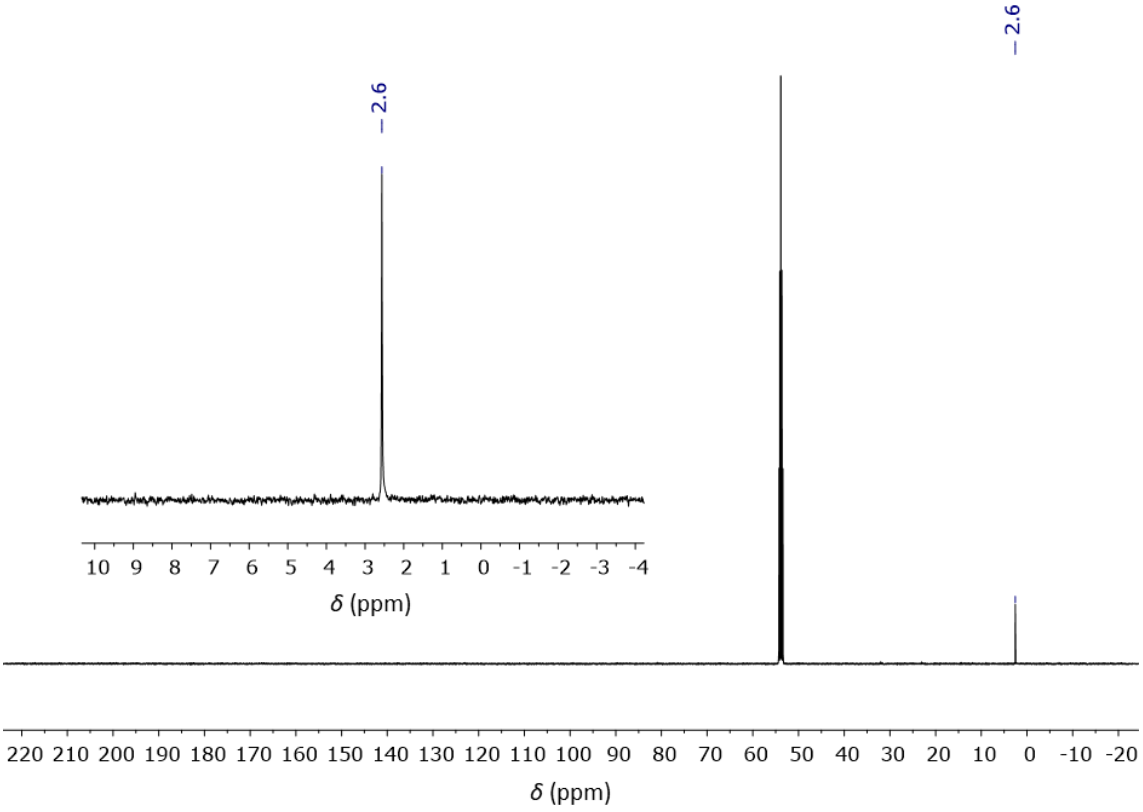

Figure S4. $^{13}C\{^{1}H\}$ NMR spectrum of **[0]** (CD_2Cl_2, 125.8 MHz).

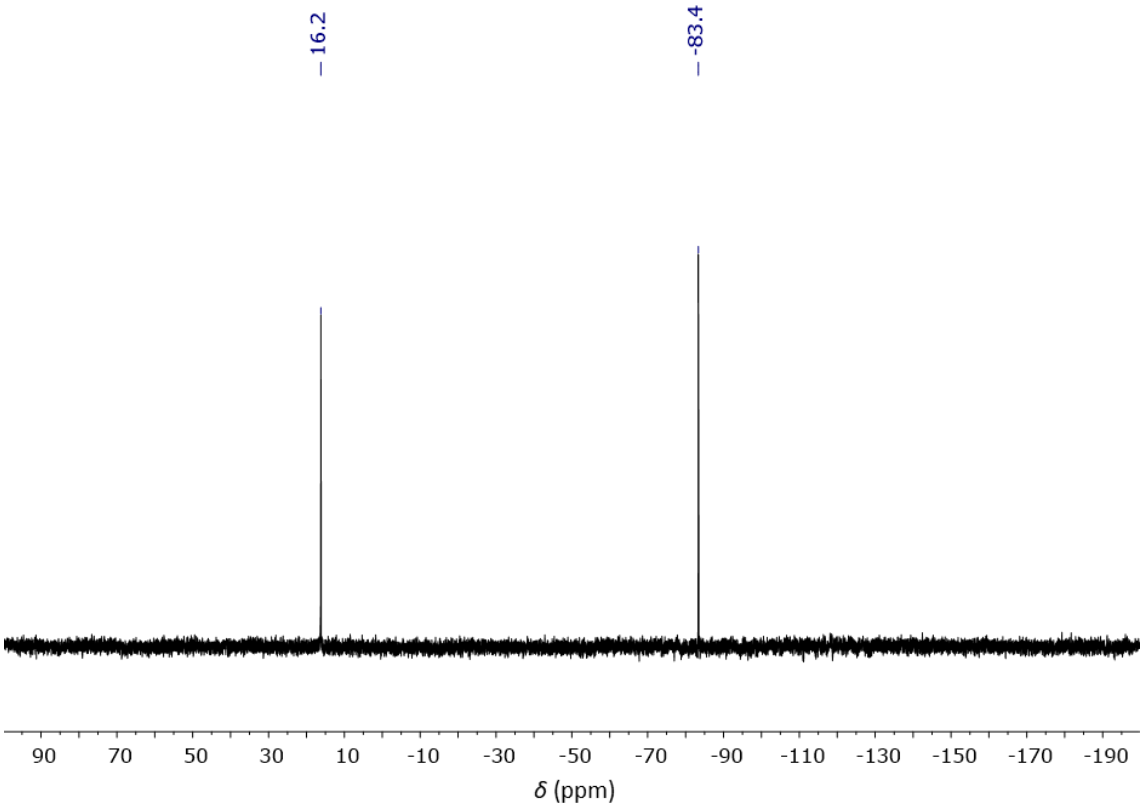

Figure S5. $^{29}Si\{^{1}H\}$ NMR spectrum of **[0]** (CD_2Cl_2, 99.4 MHz).

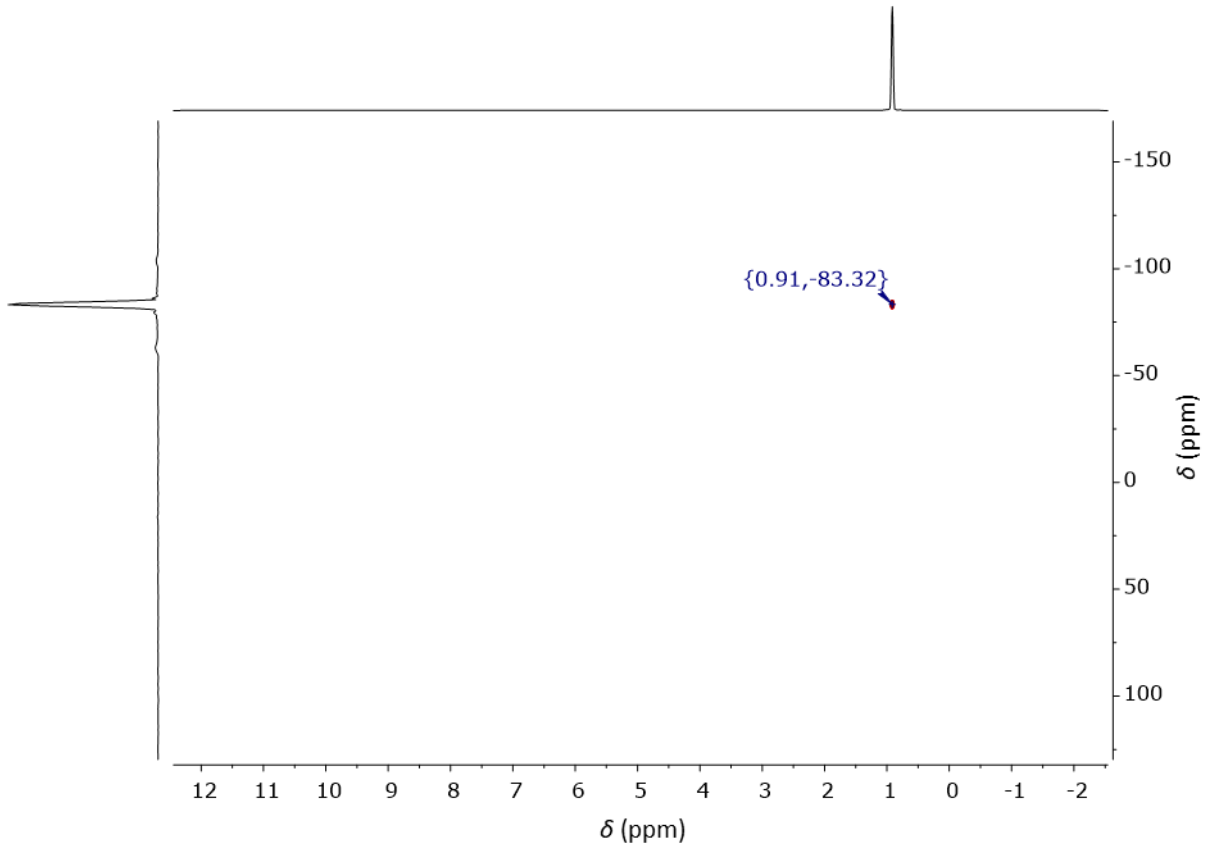

Figure S6. $^{29}Si/^{1}H$ HMBC NMR spectrum of **[0]**.

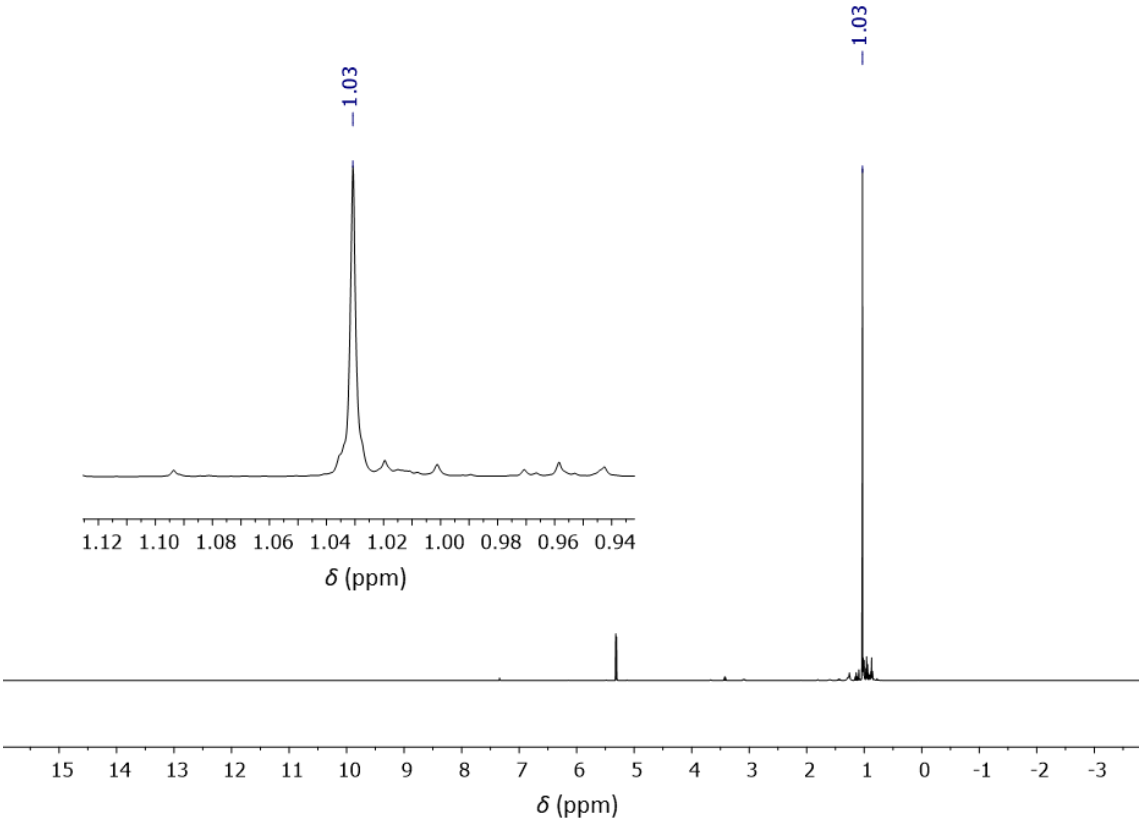

Figure S7. ^{1}H NMR spectrum of **[2]** (CD_2Cl_2, 500.2 MHz) containing traces of *n*-hexane (cf. Figure S8).

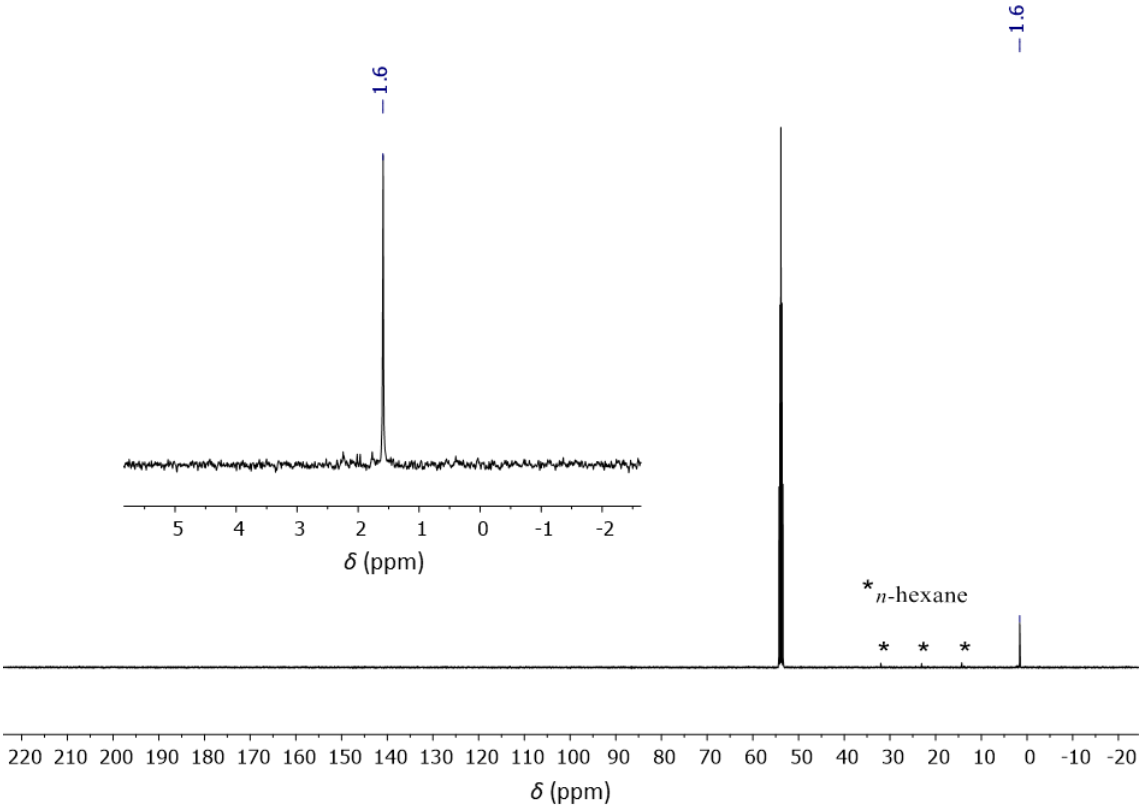

Figure S8. $^{13}C\{^{1}H\}$ NMR spectrum of **[2]** (CD_2Cl_2, 125.8 MHz); * *n*-hexane.

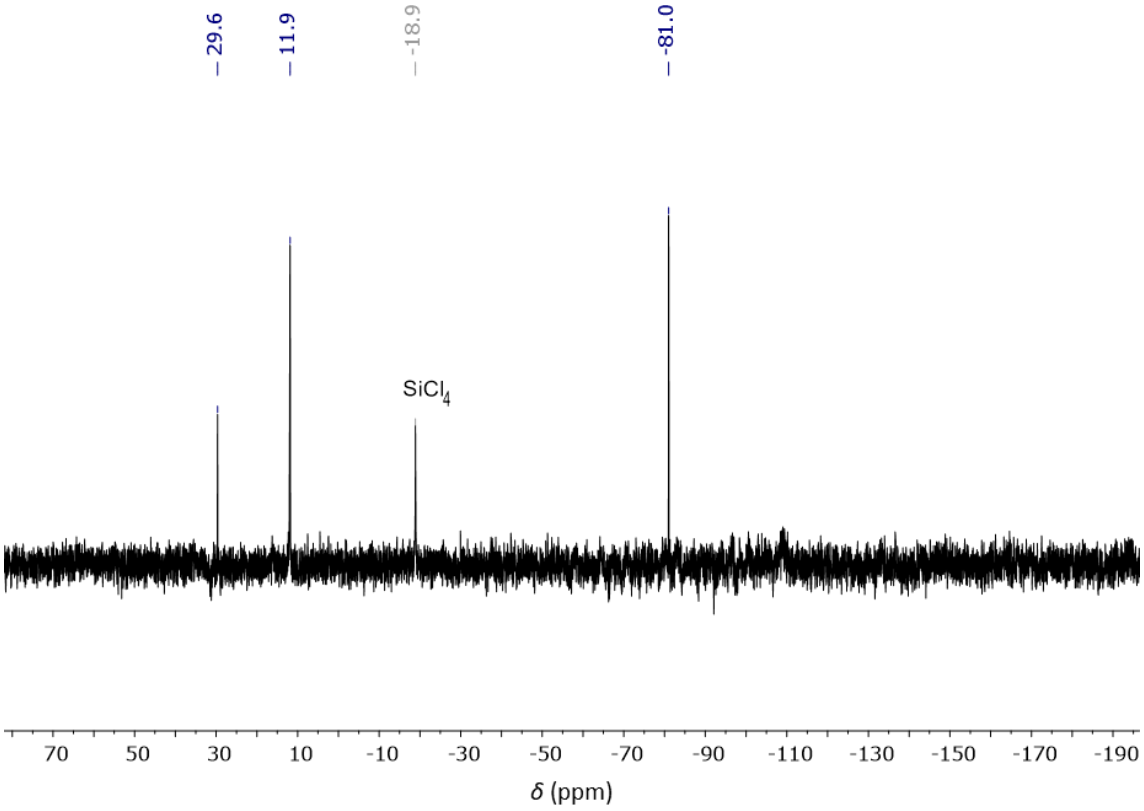

Figure S9. $^{29}Si\{^{1}H\}$ NMR spectrum of **[2]** (CD_2Cl_2, 99.4 MHz) containing $SiCl_4$ as internal standard.

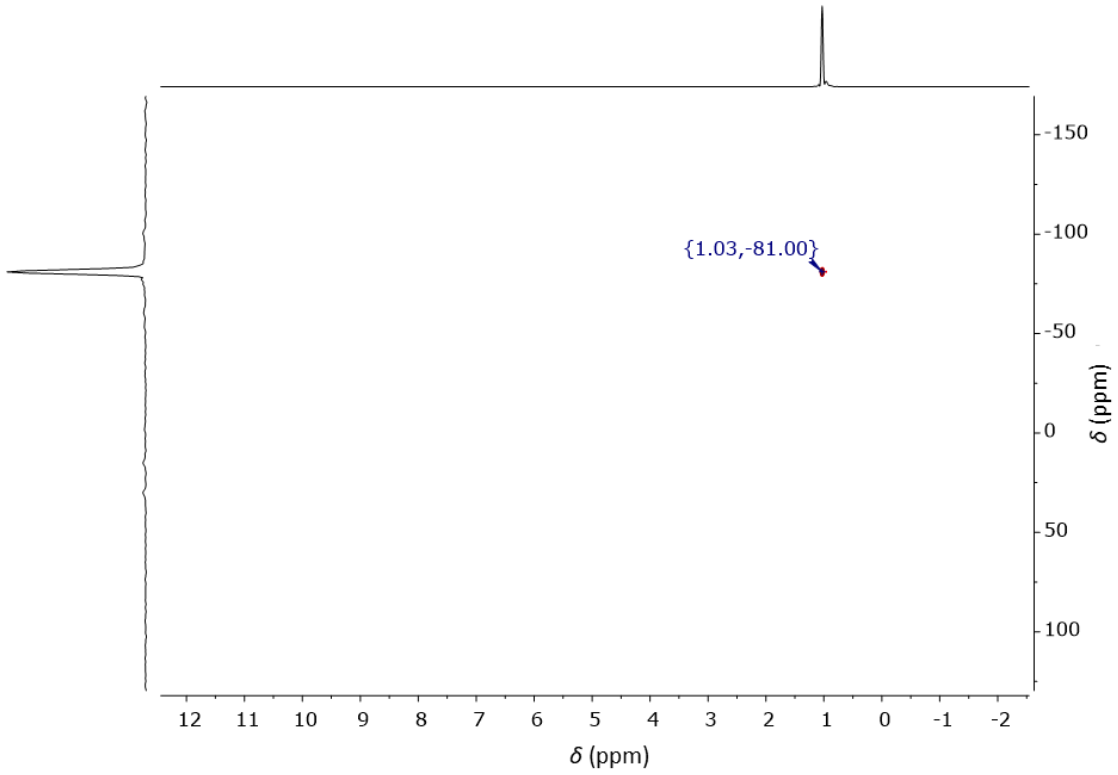

Figure S10. $^{29}Si/^{1}H$ HMBC NMR spectrum of **[2]**.

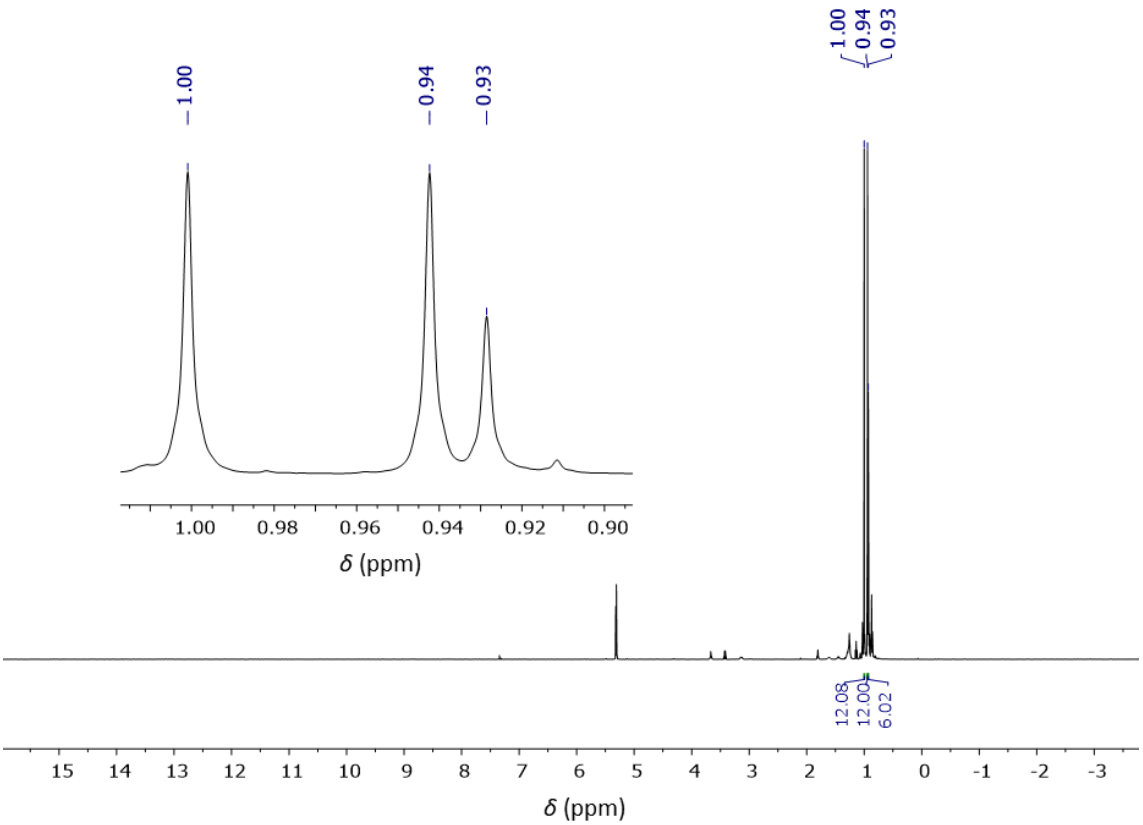

Figure S11. ^{1}H NMR spectrum of **[1]** (CD_2Cl_2, 500.2 MHz) containing traces of *n*-hexane (cf. Figure S12).

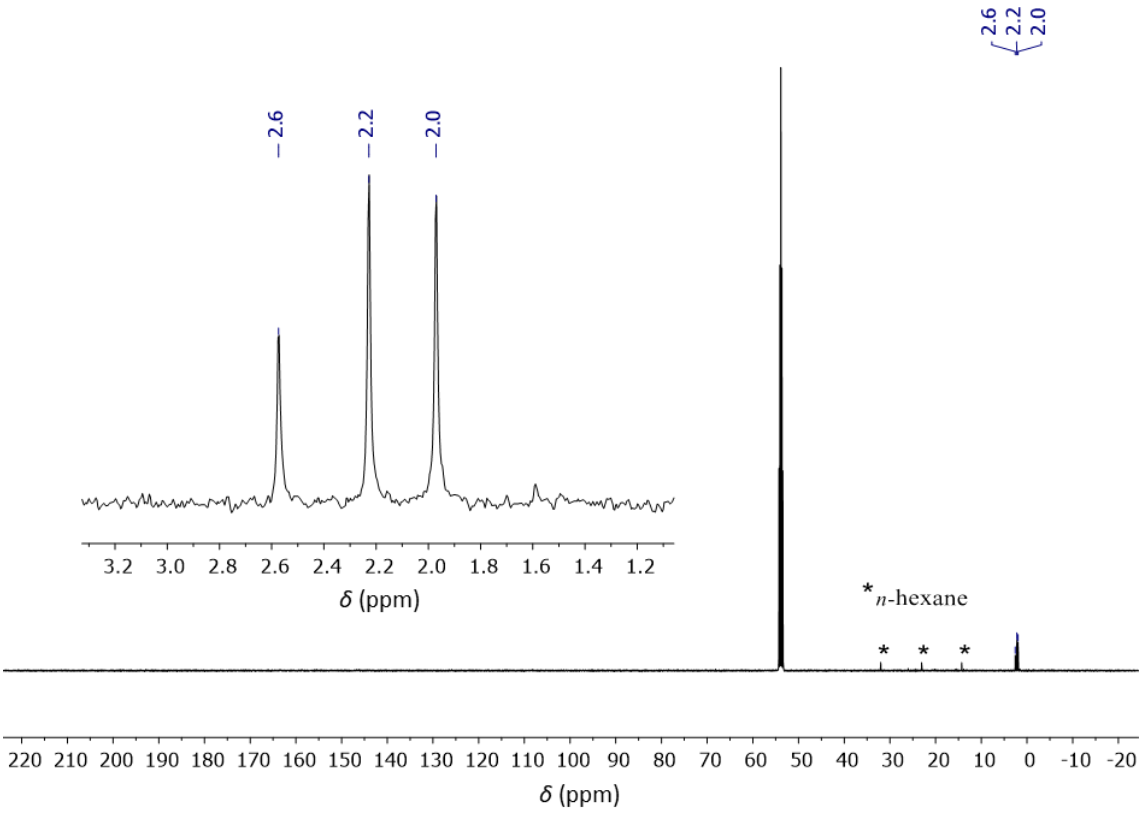

Figure S12. $^{13}C\{^{1}H\}$ NMR spectrum of **[1]** (CD_2Cl_2, 125.8 MHz); * *n*-hexane.

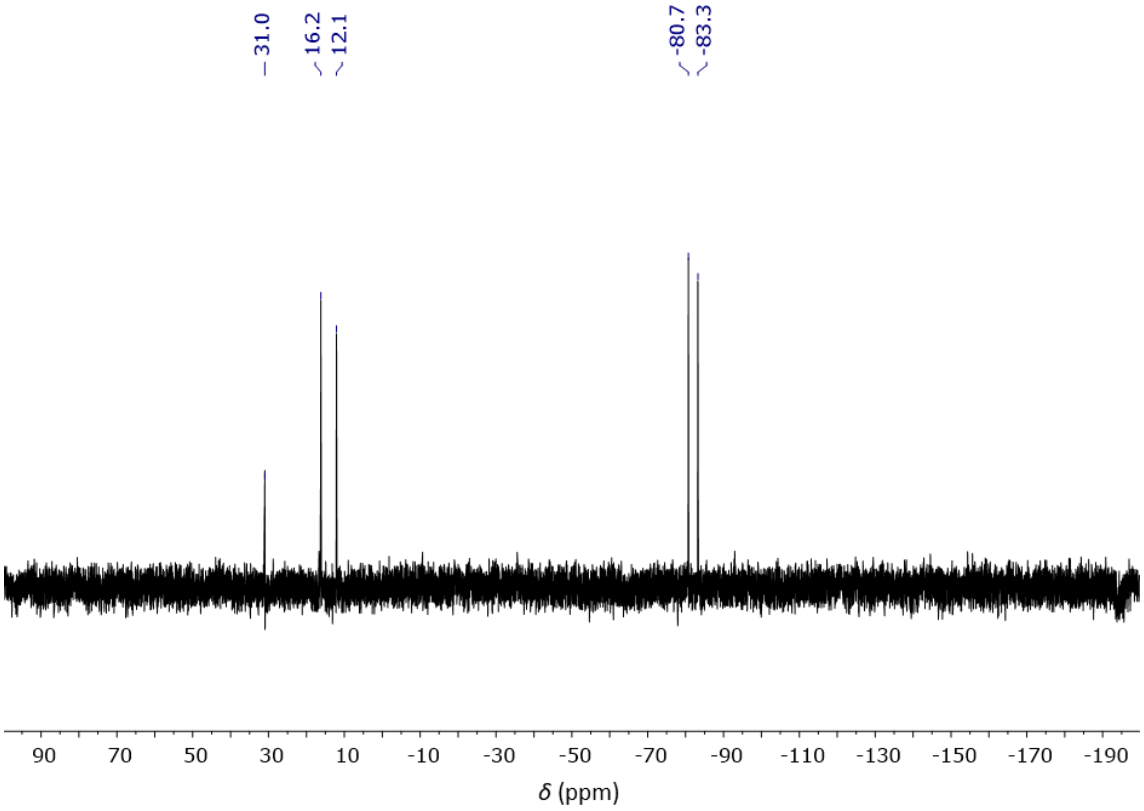

Figure S13. $^{29}Si\{^{1}H\}$ NMR spectrum of **[1]** (CD_2Cl_2, 99.4 MHz).

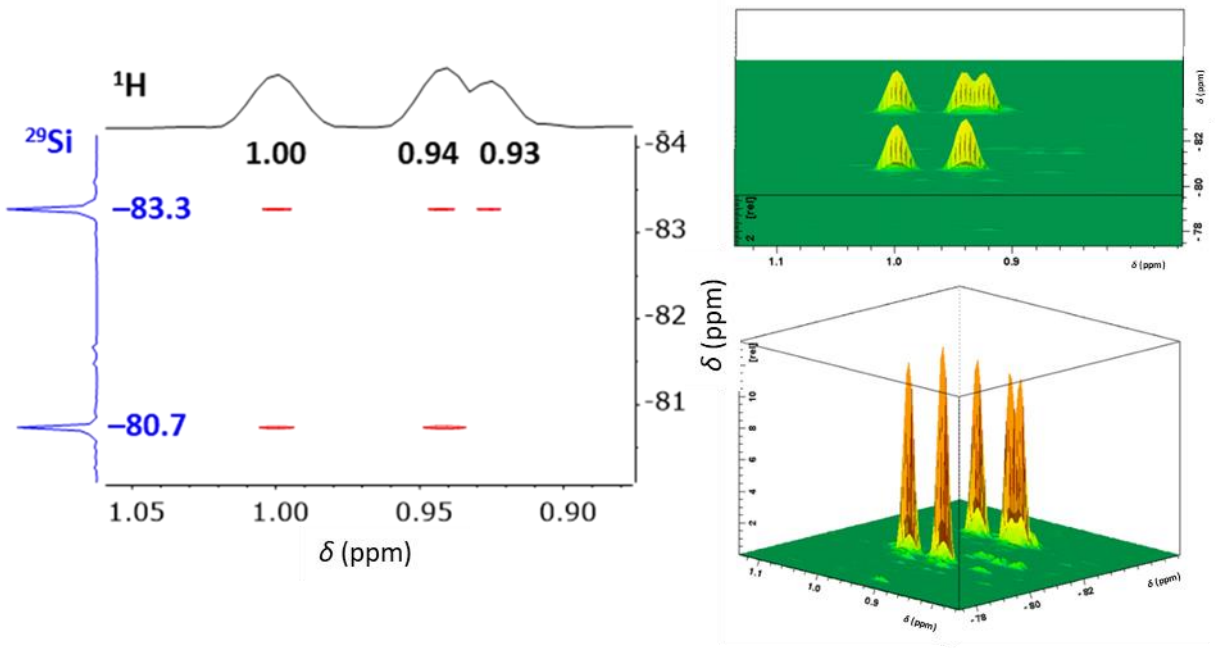

Figure S14. $^{29}Si/^{1}H$ HMBC NMR spectrum of **[1]** with cross peaks in very high resolution (left) and two perspectives of the 3D projection (top and bottom right).

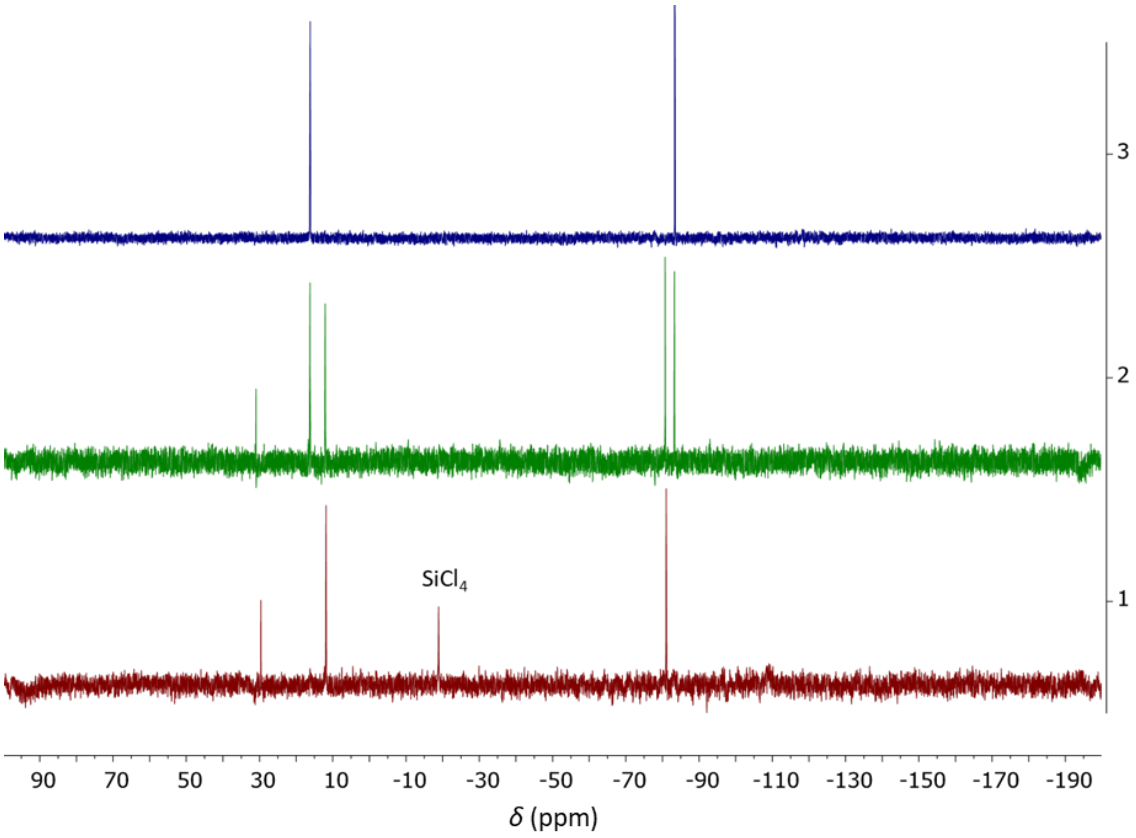

Figure S15. $^{29}Si\{^{1}H\}$ NMR spectra of **[0]** (top, blue), **[1]** (middle, green) and **[2]** (bottom, red; resonance at –18.9 ppm assignable to $SiCl_4$).

3. UV/Vis absorption spectra

Since the solvent CH_2Cl_2 is not suitable for UV/Vis measurements at wavelengths of < 230 nm, measurements of **[0]**, **[1]**, and **[2]** were performed in cyclohexane.

Table S2. Photophysical data of the compounds **[0]**, **[1]**, and **[2]**. Measurements were performed in cyclohexane.

	λ_{max} [nm] (ε [$mol^{-1}dm^3cm^{-1}$])	λ_{onset} [nm][a]	E_G^{opt} [eV][b]
[0]	234 (1.3×10^5) 205 (1.0×10^5)	285	4.35
[1]	228 (0.4×10^5)	280	4.43
[2]		272	4.56

[a] Each onset wavelength (λ_{onset}) was determined by constructing a tangent on the point of inflection of the bathochromic slope of the most red-shifted absorption maximum. [b] Optical band gap E_G^{opt} = (1240 eV·nm) / λ_{onset}.

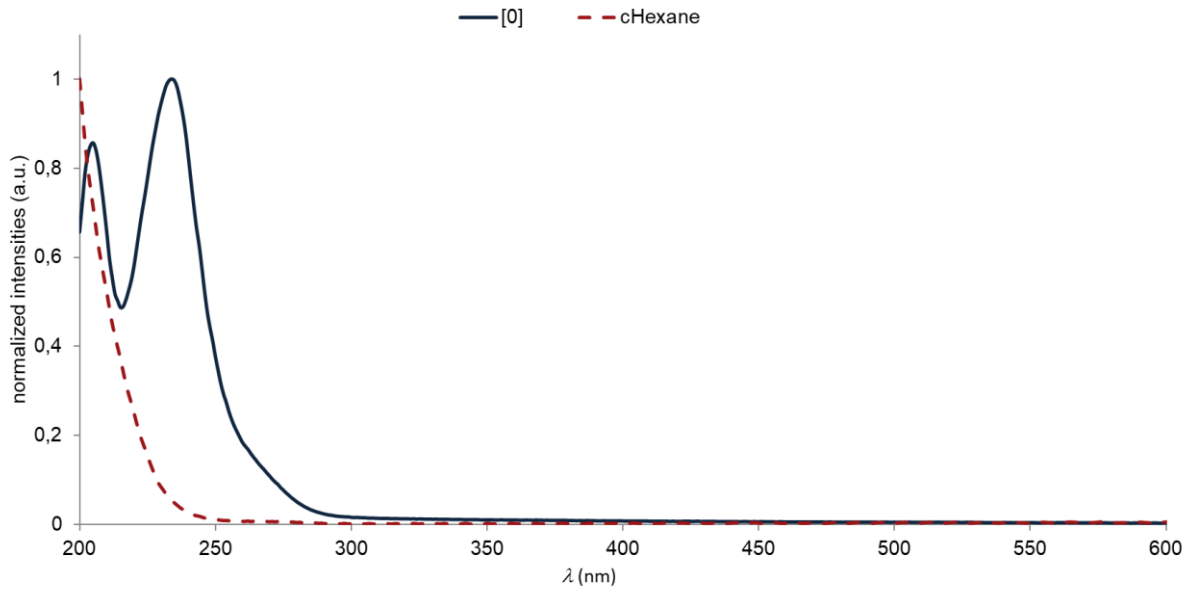

Figure S16. Normalized UV/Vis absorption spectrum of **[0]** in comparison to pure cyclohexane (dashed line).

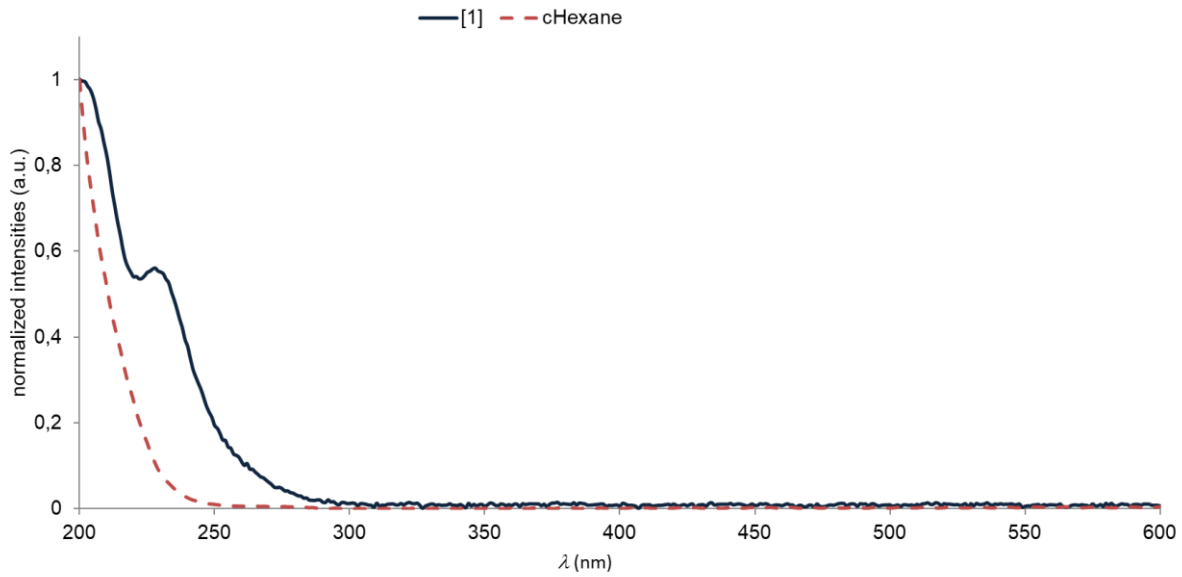

Figure S17. Normalized UV/Vis absorption spectrum of **[1]** in comparison to pure cyclohexane (dashed line).

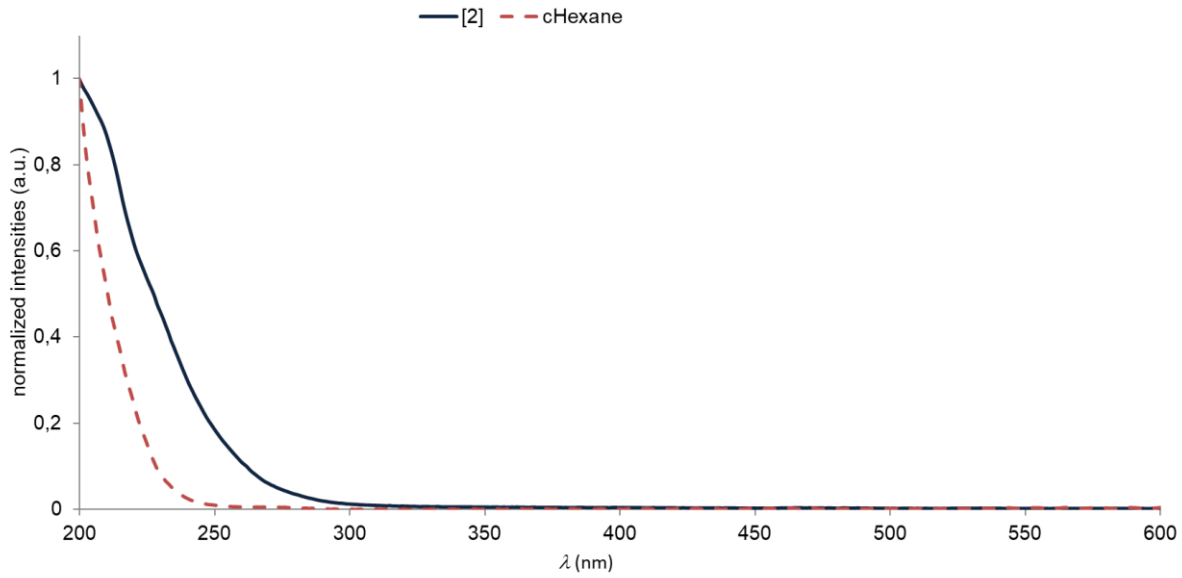

Figure S18. Normalized UV/Vis absorption spectrum of **[2]** in comparison to pure cyclohexane (dashed line).

4. Single-crystal X-ray analysis of [0], [1], and [2]

Data for all structures were collected on a STOE IPDS II two-circle diffractometer with a Genix Microfocus tube with mirror optics using MoK_α radiation (λ = 0.71073 Å). The data were scaled using the frame-scaling procedure in the *X-AREA* program system.[2] The structures were solved by direct methods using the program *SHELXS*[3] and refined against F^2 with full-matrix least-squares techniques using the program *SHELXL*.[3]

CCDC files CCDC 2091220 (**[0]**), CCDC 2091221 (**[1]**), and CCDC 2091222 (**[2]**) contain the supplementary crystallographic data for this paper and can be obtained free of charge from The Cambridge Crystallographic Data Centre via www.ccdc.cam.ac.uk/data_request/cif.

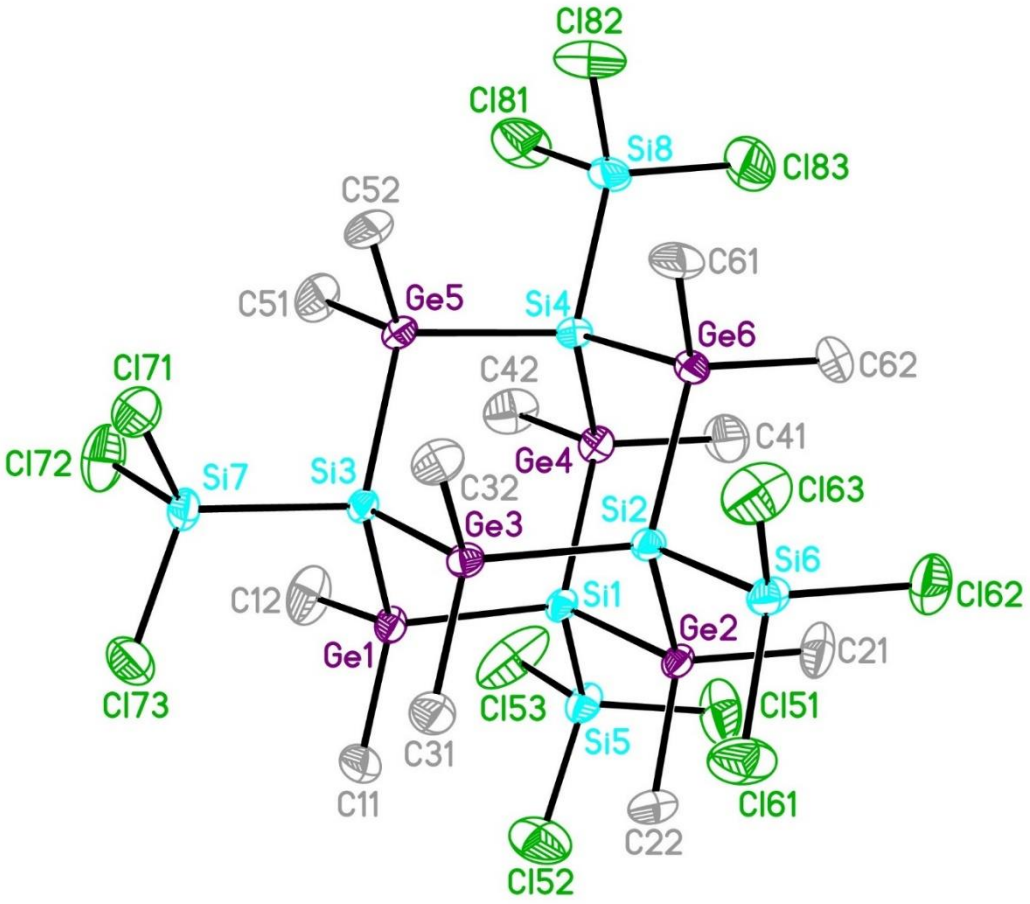

Figure S19. Molecular structure of **[0]**·CH_2Cl_2 in the solid state. Displacement ellipsoids are shown at the 50% probability level. Hydrogen atoms and the CH_2Cl_2 molecule are omitted for clarity. For selected bond lengths [Å] and bond angles [°] see Table S3.

In **[0]**·CH_2Cl_2, the heteroadamantane contains no symmetry element. The Cl and H atoms of the co-crystallized CH_2Cl_2 molecule are disordered over two sets of sites with site occupation factors of 0.542(8) for the major occupied sites.

Table S3. Ranges of selected bond lengths [Å] and bond angles [°] of **[0]**·CH_2Cl_2.

bond length/ angle	minimal value	maximal value	average
Ge–Si	Ge(5)–Si(4) = 2.3915(13)	Ge(1)–Si(1) = 2.3993(13)	2.395
Si–Si	Si(1)–Si(5) = 2.3139(16)	Si(2)–Si(6) = 2.3226(16)	2.319
Si–Cl	Si(5)–Cl(53) = 2.031(2)	Si(8)–Cl(81) = 2.055(2)	2.042
Ge–C	Ge(3)–C(32) = 1.944(4)	Ge(1)–C(12) = 1.968(5)	1.958
Ge–Si–Ge	Ge(1)–Si(3)–Ge(3) = 108.82(5)	Ge(5)–Si(3)–Ge(1) = 113.94(5)	111.63
Si–Si–Ge	Si(1)–Ge(2)–Si(2) = 103.86(4)	Si(3)–Ge(5)–Si(4) = 105.65(4)	104.93

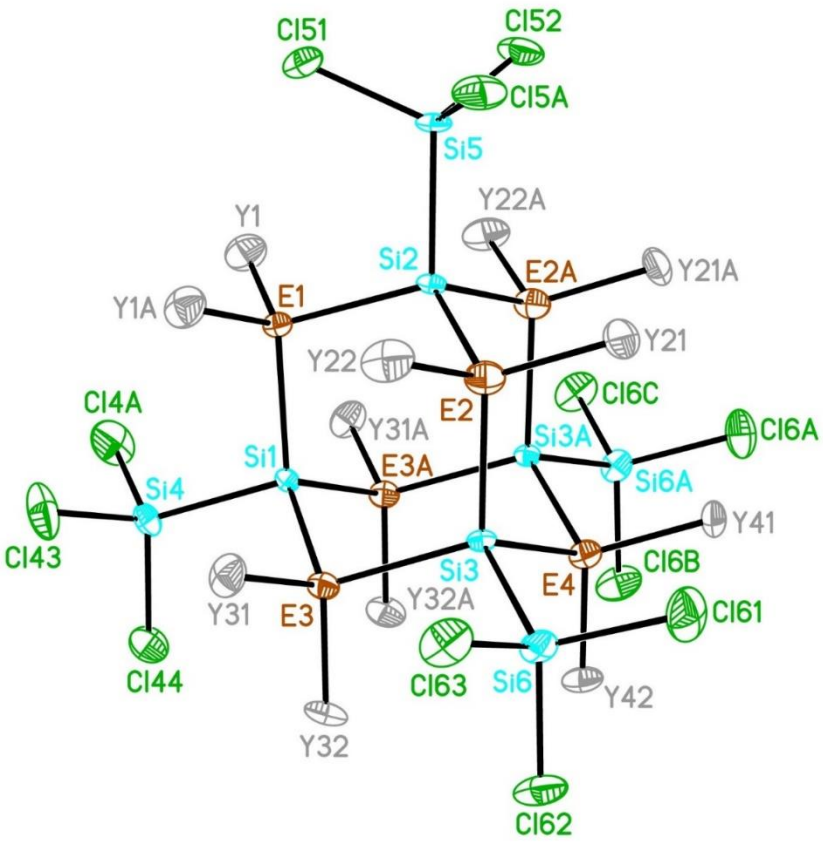

Figure S20. Molecular structure of **[1]** in the solid state. Displacement ellipsoids are shown at the 50% probability level. Hydrogen atoms are omitted for clarity. EY_2 groups are either $GeMe_2$ or $SiCl_2$. Selected bond lengths [Å]: Si(1)–Si(4) = 2.317(4) (min), Si(2)–Si(5) = 2.342(4) (max), 2.327 (average Si–Si), Si(4)–Cl(43) = 2.038(3) (min), Si(5)–Cl(52) = 2.046(3) (max), 2.042 (average Si–Cl). Symmetry transformation used to generate equivalent atoms: (A) = (B) = (C): –x+1, y, z.

The molecule of **[1]** is located on a mirror plane running through E(1), E(4), Si(1), and Si(2). The $GeMe_2$ groups are disordered with $SiCl_2$ and therefore labeled EY_2. $GeMe_2$ and $SiCl_2$ groups that are located on the same site were refined with the same coordinates and displacement parameters (for Ge/Si or C/Cl). The sum of site occupation factors (sof) of all $GeMe_2$ groups was constrained to 5. The site occupation factors of the $GeMe_2$ groups refined to 0.931(4) for E(1), 0.724(2) for E(2), 0.898(2) for E(3), and 0.824(4) for E(4). The site occupation factors of the corresponding $SiCl_2$ groups are 1-sof($GeMe_2$). If the number of $GeMe_2$ groups is changed from 5 to 4 or 6, the figures-of-merit become worse (Table S4).

The absolute structure could be determined (Flack-x-parameter -0.015(16)).

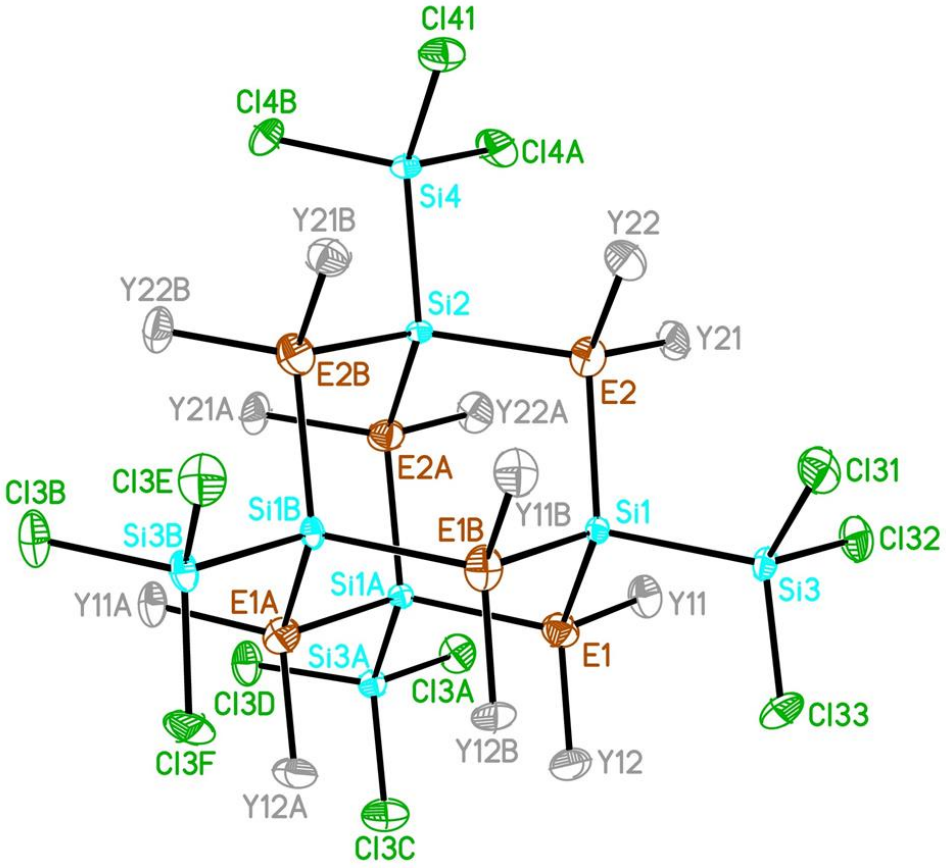

Figure S21. Molecular structure of **[2]** in the solid state. Displacement ellipsoids are shown at the 50% probability level. Hydrogen atoms are omitted for clarity. EY_2 groups are either $GeMe_2$ or $SiCl_2$. Selected bond lengths [Å]: Si(2)–Si(4) = 2.320(2) (min), Si(1)–Si(3) = 2.3260(11) (max), 2.323 (average Si–Si), Si(4)–Cl(41) = 2.0364(10) (min), Si(3)–Cl(33) = 2.0384(13) (max), 2.037 (average Si–Cl). Symmetry transformations used to generate equivalent atoms: (A) = (C) = (D): –y+1, x–y, z, (B) = (E) = (F): –x+y+1, –x+1, z.

The molecule of **[2]** is located on a three-fold rotation axis running through Si(2) and Si(4). The $GeMe_2$ groups are disordered with $SiCl_2$ and therefore labeled EY_2. $GeMe_2$ and $SiCl_2$ groups that are located on the same site were refined with the same coordinates and displacement parameters (for Ge/Si or C/Cl). The sum of site occupation factors (sof) of all $GeMe_2$ groups was constrained to 4. The site occupation factors of the $GeMe_2$ groups refined to 0.6676(8) for E(1) and 0.6657(8) for E(2). The site occupation factors of the corresponding $SiCl_2$ groups are 1-sof($GeMe_2$). If the number of $GeMe_2$ groups is increased from 4 to 5 or 6, the figures-of-merit become worse (Table S4).

The contribution of the solvent was suppressed using the *SQUEEZE* routine in *PLATON*.[4]

Table S4. Figures-of-merit of the crystal structures of **[1]** and **[2]** after refinement assuming 4, 5, and 6 $GeMe_2$ (and correspondingly 2, 1, and 0 $SiCl_2$) groups in the backbone.

crystal structure	number of $GeMe_2$ groups	*R*1	*wR*2	e(max) [e·Å^{-3}]	e(min) [e·Å^{-3}]	GooF
[1]	4	0.0597	0.1332	1.026	–1.002	1.238
	5	**0.0518**	**0.1138**	**1.029**	**–0.803**	**1.084**
	6	0.0620	0.1420	1.312	–1.336	1.394
[2]	**4**	**0.0466**	**0.1015**	**0.693**	**–0.653**	**1.259**
	5	0.0640	0.1471	1.295	–1.161	1.922
	6	0.1070	0.2572	5.134	–1.965	3.545

Table S5. Crystal data and structure refinement for **[0]**·CH_2Cl_2.

Identification code	wa3079	
Empirical formula	C_{13} H_{38} Cl_{14} Ge_6 Si_8	
Formula weight	1350.99	
Temperature	173(2) K	
Wavelength	0.71073 Å	
Crystal system	Triclinic	
Space group	*P*-1	
Unit cell dimensions	*a* = 12.3759(6) Å	α = 80.448(4)°.
	b = 12.4990(6) Å	β = 88.753(4)°.
	c = 16.3541(8) Å	γ = 85.722(4)°.
Volume	2487.6(2) $Å^3$	
Z	2	
Density (calculated)	1.804 Mg/m^3	
Absorption coefficient	4.536 mm^{-1}	
F(000)	1316	
Crystal size	0.210 × 0.180 × 0.060 mm^3	
Theta range for data collection	3.309 to 25.727°.	
Index ranges	–12<=h<=15, –15<=k<=15, –19<=l<=19	
Reflections collected	34472	
Independent reflections	9286 [*R*(int) = 0.0716]	
Completeness to theta = 25.000°	99.7 %	
Absorption correction	Semi-empirical from equivalents	
Max. and min. transmission	1.000 and 0.350	
Refinement method	Full-matrix least-squares on F^2	
Data / restraints / parameters	9286 / 0 / 389	
Goodness-of-fit on F^2	1.018	
Final *R* indices [I>2sigma(I)]	*R1* = 0.0504, *wR2* = 0.1315	
R indices (all data)	*R1* = 0.0627, *wR2* = 0.1415	
Largest diff. peak and hole	1.143 and –0.951 e·$Å^{-3}$	

Table S6. Crystal data and structure refinement for **[1]**.

Identification code	wa2935	
Empirical formula	C_{10} H_{30} Cl_{14} Ge_5 Si_9	
Formula weight	1262.40	
Temperature	173(2) K	
Wavelength	0.71073 Å	
Crystal system	Orthorhombic	
Space group	*Cmc*2_1	
Unit cell dimensions	*a* = 18.6137(6) Å	α = 90°.
	b = 19.6940(8) Å	β = 90°.
	c = 12.3165(5) Å	γ = 90°.
Volume	4515.0(3) Å^3	
Z	4	
Density (calculated)	1.857 Mg/m^3	
Absorption coefficient	4.369 mm^{-1}	
F(000)	2456	
Crystal size	0.190 × 0.130 × 0.040 mm^3	
Theta range for data collection	3.291 to 27.713°.	
Index ranges	–23<=h<=24, –25<=k<=25, –16<=l<=15	
Reflections collected	23976	
Independent reflections	5349 [*R*(int) = 0.0518]	
Completeness to theta = 25.000°	99.6 %	
Absorption correction	Semi-empirical from equivalents	
Max. and min. transmission	1.000 and 0.495	
Refinement method	Full-matrix least-squares on F^2	
Data / restraints / parameters	5349 / 1 / 191	
Goodness-of-fit on F^2	1.085	
Final *R* indices [I>2sigma(I)]	*R1* = 0.0430, *wR2* = 0.1065	
R indices (all data)	*R1* = 0.0518, *wR2* = 0.1138	
Absolute structure parameter	–0.015(15)	
Largest diff. peak and hole	1.029 and –0.803 e·Å^{-3}	

Table S7. Crystal data and structure refinement for **[2]**.

Identification code	wa2970	
Empirical formula	$C_8 H_{24} Cl_{16} Ge_4 Si_{10}$	
Formula weight	1258.73	
Temperature	173(2) K	
Wavelength	0.71073 Å	
Crystal system	Trigonal	
Space group	*R*-3:H	
Unit cell dimensions	a = 17.3328(3) Å	α = 90°.
	b = 17.3328(3) Å	β = 90°.
	c = 28.6818(7) Å	γ = 120°.
Volume	7462.3(3) $Å^3$	
Z	6	
Density (calculated)	1.681 Mg/m^3	
Absorption coefficient	3.504 mm^{-1}	
F(000)	3672	
Crystal size	0.180 × 0.150 × 0.120 mm^3	
Theta range for data collection	2.350 to 27.661°.	
Index ranges	–22<=h<=22, –22<=k<=22, –37<=l<=37	
Reflections collected	56306	
Independent reflections	3832 [*R*(int) = 0.0524]	
Completeness to theta = 25.000°	99.8 %	
Absorption correction	Semi-empirical from equivalents	
Max. and min. transmission	1.000 and 0.745	
Refinement method	Full-matrix least-squares on F^2	
Data / restraints / parameters	3832 / 1 / 117	
Goodness-of-fit on F^2	1.260	
Final *R* indices [I>2sigma(I)]	*R1* = 0.0437, *wR2* = 0.1003	
R indices (all data)	*R1* = 0.0466, *wR2* = 0.1015	
Largest diff. peak and hole	0.693 and –0.653 $e \cdot Å^{-3}$	

5. References

[1] G. R. Fulmer, A. J. M. Miller, N. H. Sherden, H. E. Gottlieb, A. Nudelman, B. M. Stoltz, J. E. Bercaw, K. I. Goldberg, *Organometallics* **2010**, *29*, 2176–2179.

[2] Stoe & Cie, X-AREA. Diffractometer control program system. Stoe & Cie, Darmstadt, Germany, **2002**.

[3] G. M. Sheldrick, *Acta Crystallogr. Sect. A Found. Crystallogr.* **2008**, *64*, 112–122.

[4] A. L. Spek, *Acta Crystallogr. Sect. D Biol. Crystallogr.* **2009**, *65*, 148–155.